Chapter 4

Modeling of a Parabolic Dish and Trough solar Concentrators

In this chapter, performance model has been developed for parabolic dish and trough type solar collector systems using a numerical approach. Optical, thermal and energetic modeling of the present experimental setup has been analysed. Performance model developed is validated with the experimental results which confirm the validity and reliability of the data under Varanasi climatic zone. Experimental results have also been compared with the data obtained from the SNL test results (1994). Heat loss analysis of solar receiver and the effect of various enviromental parameters on it were investigated. Determination of exergy loss, exergy destruction, optical, thermal and exergetic efficiency has also been investigated.

4.1 Modeling of a Parabolic Trough solar Concentrator

The linear parabolic concentrators are used to focus sunlight to heat the pumped heat transfer fluid in the absorber as shown in Fig. 3.3. The excellent light transmittance and heat durability borosilicate glass envelopes are used to maintain the vacuum space between two concentric glass annulus in order to reduce heat loss and prevent corroding [144]. Zhai Rongrong et al. [145] suggests that the luminousness might be increased by enhancing the optical performance of glass envelope. Performance of luminousness and anticorrosion of glass envelope should be very good because there will be no vacuum when the glass is corroded. Heat and mass balance equation has been given in next section.

This section includes the numerical modeling and heat transfer analysis of helical coil solar cavity receiver. Fig. 4.1 illustrates the mechanism of heat transfer between the

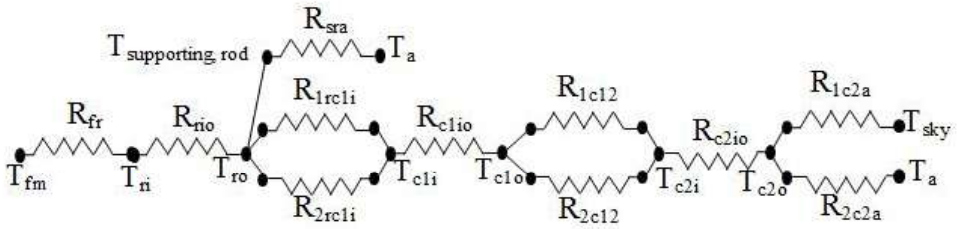

Figure 4.1: Thermal resistance model for a cross section of a double glazing helical coil solar receiver

heat transfer fluid, HTF and the ambient.

Solar radiation passes through the evacuated glass covers is absorbed by selective coating on the absorber tube. The inner wall of the receiver absorbs partial energy from the coatings by conduction (R_{rio}) and the same is transferred to HTF by convection (R_{fr}). The losses take place by the absorbed energy is transmitted to the 1^{st} glass cover by convection/conduction (R_{1rc1i}) and radiation (R_{2rc1i}) and is further lost through metallic receiver ends by conduction (R_{sra}). Further, loss of the conducted energy (R_{c1io}) by the 1st glass cover is transmitted to the 2^{nd} glass cover by convection (R_{1c12}) and radiation (R_{2c12}) and the energy absorbed by the glass envelope are collectively lost to surroundings by convection (R_{1c2a}) between glass envelop and ambient and radiation (R_{2c2a}) between glass envelop and the sky. The numerical modeling of heat losses from HTF to ambient has been reported in details what will be given in the next section.

4.1.1 One Dimensional Energy Balance Model

In a solar PTC or in any solar concentrating collector, the absorber of the system plays a vital role in the collection of solar energy. T_o achieve higher efficiency of the solar collector, there should be minimum thermal losses from the absorber. Therefore, the overall heat loss coefficient is of great importance to the solar absorber and it includes conduction, convection and radiation heat losses. The various heat energy gain and loss that occurred in the receiver section of the solar PTC are depicted in Fig. 4.2. Q_1 to Q_5corresponds to the phenomenon of heat transfer from the source, sunlight in to useful heat gain by the heat transfer fluid. Q_6 to Q_{14} depicts the various losses that occur in a solar PTC system. Solar radiation intensity passes through the evacuated glass covers

Q_3 is absorbed by selective coating on the absorber tube. The inner wall of the receiver absorbs partial energy from the coatings by conduction Q_4 and the same is transferred to HTF by convection Q_5. The losses take place by the absorbed energy is transmitted to the 1^{st} glass cover by convection Q_6 and radiation Q_7 and is further lost through metallic receiver ends by conduction Q_{14}. Further, loss of the conducted energy Q_8 by the 1^{st} glass cover is transmitted to the 2^{nd} glass cover by convection Q_9 and radiation Q_{10} and the energy absorbed by the glass envelope are collectively lost to surroundings by convection Q_{12} and radiation Q_{13}.

$$Q_4 = Q_5 \tag{4.1}$$

$$Q_3 = Q_4 + Q_6 + Q_7 + Q_{14} \tag{4.2}$$

$$Q_6 + Q_7 = Q_8 \tag{4.3}$$

$$Q_2 + Q_8 = Q_9 + Q_{10} \tag{4.4}$$

$$Q_9 + Q_{10} = Q_{11} \tag{4.5}$$

$$Q_1 + Q_{11} = Q_{12} + Q_{13} \tag{4.6}$$

$$Q_{Heat\,loaa} = Q_{12} + Q_{13} + Q_{14} \tag{4.7}$$

4.1.2 Convection Heat Transfer between the HTF and the Absorber

A typical double glazing helical coil solar cavity receiver is shown in Fig. (4.3). In this figure, d is the diameter of the coiled tube, R_c is the curvature radius of the coil, D_{1_i}, $D_{1o}$and D_{2i}, $D_{2o}$are the inner and outer diameters of 1^{st} and 2^{nd} glazing cover respectively over helical coil absorber and b is the coil pitch. The curvature ratio, δ, is defined as the coil-to-tube diameter ratio, $d/2R_c$, and the non-dimensional pitch, γ, is defined as $b/2\pi R_c$. M.R. Salimpour (2009) [146] suggests four important dimensionless parameters of helical coiled tube namely, Reynolds number (Re_i), Nusselt number (Nu_i), Dean number (De), and Helical number (He) which are defined as follow:

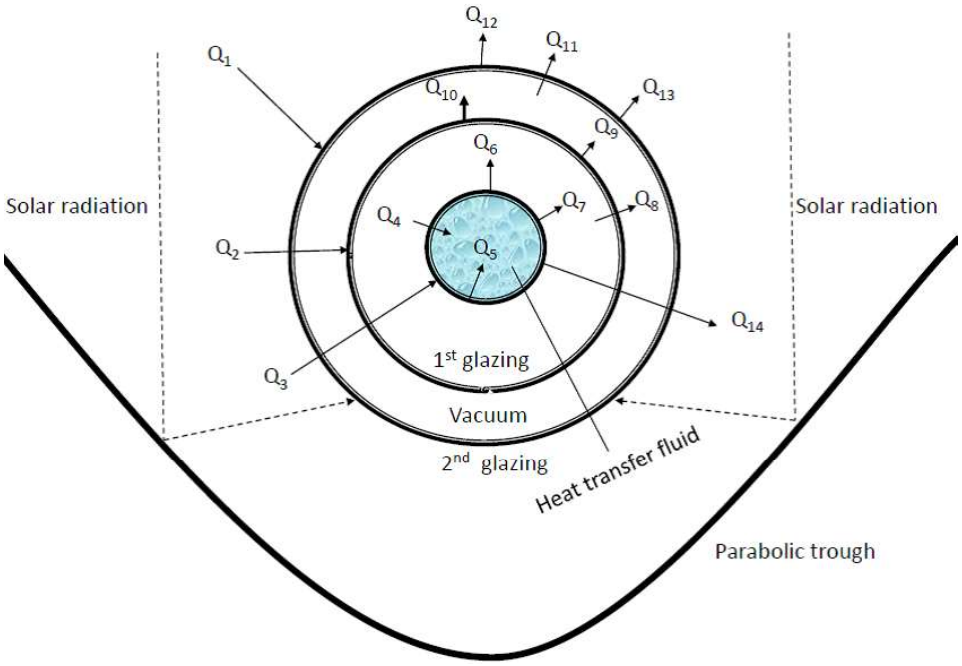

Figure 4.2: shows the heat gain and loss through parabolic trough concentrator

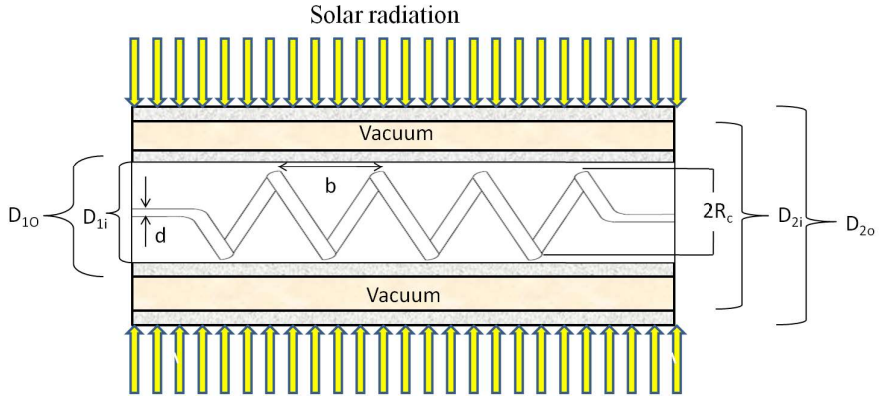

Figure 4.3: Schematic view of typical double glazing helical coil solar cavity receiver

$$Re_i = \frac{\rho v_i d_i}{\mu}; \qquad Nu = \frac{h_i d_i}{k}; \qquad De = Re_i \times \sqrt{\frac{d_i}{2R_c}}; \qquad He = \frac{De}{\sqrt{1+\gamma^2}}$$

Where v_i and h_i are the average velocity of heat transfer fluid and convective heat transfer coefficient at coil fluid interface, respectively. Now considering the region between helical coil surface and 1^{st} glazing cover, Nusselt number (Nu_o) and Reynolds number (Re_o) are defined as

$Nu_o = \frac{h_o D_{h_{1i}}}{k}$; $\qquad Re_o = \frac{\rho v_o D_{h1i}}{\mu}$

where $D_{h_{1i}} = \frac{D_{1i}^2 - 2\pi R_c d_o^2 \gamma^{-1}}{D_{1i} + 2\pi R_c d_o \gamma^{-1}}$ is the hydraulic diameter of 1^{st} glazing cover side of helical coil receiver. h_o, v_o and d_o are the convective heat transfer coefficient, average fluid velocity and outer diameter of helical coil tube, respectively. From Newton's law of cooling, the convection heat transfer from the inside surface of the absorber pipe to the HTF per unit length of absorber pipe is

$$Q = h_i d_i \pi (T_4 - T_5) \tag{4.8}$$

where

Q_5 = convection heat transfer between inner surface of absorber pipe to heat transfer fluid

h_i = HTF convection heat transfer coefficient at T_5 (W/m^2K)

d_i = inside diameter of the absorber pipe (m)

T_5 = mean (bulk) temperature of the HTF $(^\circ C)$

T_4 = inside surface temperature of absorber pipe $(^\circ C)$

In above equations, both T_4 and T_5 are independent of angular and longitudinal HCE (heat collecting element) directions, as all temperatures and properties are considered for one-dimensional energy balance model.

with

$$h_i = Nu_{d_i} \times \frac{K_5}{d_i} \tag{4.9}$$

Nu_{d_i}= Nusselt number based on d_i

K_5 =thermal conductance of the HTF at T_5 $(W/m-K)$

The Nusselt number depends on the type of flow through the receiver conduit. Flow of

heat transfer fluid (HTF) through the receiver conduit at high temperature is well within the turbulent flow region. However, during off-solar hours, the flow in the HCE (heat collecting element) may become laminar because of the higher viscosity of the HTF at lower temperatures. Therefore, to model the heat losses under all conditions, the model includes conditional statements to determine type of flow.

4.1.3 Nusselt Number Calculation

Nu is calculated by various correlations at specified conditions. In the present experiment heat transfer fluid (therminol vp-1) was pumped through the horizontal helical coil and the inside heat transfer coefficients were calculated based on the Nusselt number correlation of Rogers and Mayhew [147]. Other than Rogers and Mayhew, there are many other authors who suggested the empirical relations to find the inner heat transfer coefficients for the fluid passes through the helical coil tube.

1. Roger et al. [148]

$$Nu = 0.023 Re^{0.85} Pr^{0.4} \delta^{0.1} \tag{4.10}$$

for $Re \geq 2000$

2. M.R. Salimpour [146]

$$Nu = 0.15 De^{0.431} Pr^{1.06} \gamma^{-0.277}, \; for \; De \leq 3000 \tag{4.11}$$

3. Kalb et al. [149]

$$Nu = 0.83 De^{0.5} Pr^{0.1} \tag{4.12}$$

for $De \geq 3000$ and $0.7 \leq Pr \leq 5$

4. Xin et al. [150]

$$Nu = \left(2.153 + 0.318 De^{0.643}\right) Pr^{0.177} \tag{4.13}$$

for $20 \leq De \leq 2000$; $0.7 \leq Pr \leq 175$and $d/D \leq 0.0884$

5. Gnielinski [1976] [151] also developed the Nusselt number correlation to model the convective heat transfer from the absorber to the heat transfer fluid for turbulent pipe flow case (Reynolds number > 2300)

$$Nu_{d_i} = \frac{(f_2/8)(Re_{d_i} - 1000)Pr}{1 + 12.7\sqrt{f_2/8}\left(Pr_1^{2/3} - 1\right)}\left(\frac{Pr_1}{Pr_2}\right)^{0.11} \tag{4.14}$$

with

$$f_2 = (1.82\log_{10}(Re_{d_i}) - 1.64)^{-2} \tag{4.15}$$

where

f_2=friction factor for the inner surface of the absorber pipe

Pr_1=Prandtle number evaluated at the HTF temperature, T_5

Pr_2=Prandtle number evaluated at the absorber inner surface temperature, T_4

Now from equation (3.10), Inner heat transfer coefficient (h_i) can be calculated. In the present experimental setup, flows of heat transfer fluid through the helical coil tube is in the turbulent flow regime and hence above formulae are the best fitted formula for the flow through the helical coil solar cavity receiver.

6. Janssen and Hoogenwdoom (1978) [152]

$$Nu = 0.7Re^{0.43}Pr^{1/6}\left(\frac{d}{D}\right)^{0.07} \tag{4.16}$$

Conditions: $d = 5$ mm, 10 mm; L = 4500 mm, 5500 mm, 5800 mm; D_c = 120 mm, 420 mm, 500 mm, 620 mm; $100 \leq De \leq 830$; $20 \leq Pr \leq 450$

Although, there are various empirical relation of Nussult Numbers for the flow of fluid through helical coil tube but equation 4.13 has been adopted for the present experimental analysis. This is due to the reason that the experimental value of Nusselt Number is more closure to this equation.

4.1.4 Conduction Heat Transfer through the Absorber Wall (Q_4)

Fourier's law of conduction through a hollow cylinder as well as through helical coil tube follows the same equation only difference is that the heat transfer area is more in the case of helical coil in comparison to cylindrical tube for the same parabolic trough length. [Incropera and DeWitt 1990] [153]describes the conduction heat transfer through the absorber wall.

$$Q_4 = \frac{2\pi k_4 (T_4 - T_3)}{\ln\left(\frac{d_o}{d_i}\right)} \tag{4.17}$$

Where

Q_4= conduction heat transfer through the absorber wall

k_4= absorber thermal conductance at the average absorber temperature $(T_3 + T_4)/2$ (W/m-K)

T_4= absorber inside surface temperature (K)

T_3= absorber outside surface temperature (K)

d_i = absorber inside diameter (m)

d_o = absorber outside diameter (m)

The conduction coefficient depends on absorber material type. If copper (as in the present experimental setup) is chosen, the conduction coefficient is a constant of $400 W/m-K$ [ASM Handbook Committee 1978] [154]. Conductive resistance through the selective coating has been neglected in the present analysis.

4.1.5 Heat Transfer from the Absorber to the 1^{st} Glass Cover

Convection and radiation heat transfer occur between the helical coil absorber surface and the 1^{st} glass envelope. The convection heat transfer mechanism depends on the annulus pressure At low pressures ($<$ 1 torr), the heat transfer mechanism is molecular conduction. At higher pressures ($>$ 1 torr), the mechanism is free convection[KJCOC 1993] [155]. Knudsen number is one of the ways to determine the types of heat transfer in fluid. Knudsen number (Kn) is the ratio of the mean free path and the effective length between surfaces. When the mean free path is large as compared to the distance between the sur-

Table 4.1: Determining the Mode of Heat Transfer[155]

Mode of Heat Transfer	Determining Factor	Equations Implemented
Continuum	Kn < 0.01	Use gas conduction, natural convection or other equations
Mixed Continuum & Free Molecular	0.01 < Kn < 0.30	Use Free Molecular Heat Transfer equations with caution
Free Molecular	Kn > 0.30	Use Free Molecular Heat Transfer equations

faces, the probability of any collisions with other gas molecules is relatively low while crossing the gas molecules from one surface to other.

Table 4.1 [156]shows clearly that when the Knudsen number is greater than 0.30, the free molecular relations should be used to account for heat transfer. If the Knudsen number is less than 0.30 and greater than 0.01, then mode of heat transfer is mixed containing both free molecular heating and continuum heating. When the mean free path is significantly small compared to the effective length i.e. less than 0.01, rapid collisions among the molecules happens during the transport of heat from one surface to other and hence in this case continuum equation is predominant. The radiation heat transfer occurs because of the difference in temperatures between the outer absorber surface and the inner glass envelope surface. The radiation heat transfer calculation is simplified by assuming the glass envelope is opaque to infrared radiation and assuming gray ($\rho = \alpha$) surfaces. In the present experimental setup air is present between the absorber tube and the 1^{st} glass cover with pressure greater than that of atmospheric: air is trapped in space of finite volume and this space is at the focus of parabolic trough concentrator and pressure increases according to Charles law. Since, this is high pressure region ($Kn < 0.01$) and hence continuum equation should be used in this region.

4.1.6 Convection Heat Transfer (Q_6)

When the helical coil solar receiver annulus is under the pressure greater than atmospheric pressure without flow of fluid, the convection heat transfer between the absorber and glass

envelope can be solved by using continuum equation i.e. free convection heat transfer equation.

$$Q_6 = h_o d_o \pi \left(T_3 - T_{g_i}\right) \tag{4.18}$$

Where

Q_6 = convection heat transfer between receiver and 1^{st} glass cover per unit length of receiver

d_o = absorber outside diameter (m)

T_3 = absorber outside surface temperature (K)

$T_{g_{1i}}$ = inner surface temperature of 1^{st} glass cover (K)

4.1.7 Radiation Heat Transfer (Q_7)

The equation (4.19) has been derived with several assumptions: nonparticipating gas in the annulus, gray, diffuse and opaque enclosures and long concentric isothermal cylinders. But neither the glass cover nor the selective coatings on helical coil are gray, and the glass cover is not completely opaque for the entire thermal radiation spectrum [157]. However, any errors associated with the assumptions should be relatively small.

$$Q_7 = \frac{\sigma \pi d_o \left(T_3^4 - T_{g1i}^4\right)}{\frac{1}{\varepsilon} + \left(\frac{d_o}{D_{1i}}\right)\left(\frac{1-\varepsilon_{g_{1i}}}{\varepsilon_{g_{1i}}}\right)} \tag{4.19}$$

Where

Q_7 =radiation heat transfer between receiver and 1^{st} glass cover per unit length of receiver

D_{1i} =inner diameter of 1^{st} glass cover (m)

ε_3 = emissivity of receiver

$\varepsilon_{g_{1i}}$ =emissivity of 1^{st} glass cover

4.1.8 Heat Transfer from the 1st Glass Cover to 2nd Glass

4.1.8.1 Convection Heat Transfer (Q_9)

When the space between the 1^{st} glass cover and the 2nd glass cover is under vacuum (pressure less than $133.322\,Pa$), the convection heat transfer occur by free-molecular

convection and can be calculated using the correlation suggested by Ratzel et al [158].

$$Q_7 = \pi D_{lo} h_{12} (T_{1o} - T_{g2i}) \tag{4.20}$$

with

$$h_{12} = \frac{k_{std}}{\frac{D_{1o}}{2\ln(D_{2i}/D_{1o})} + b\lambda\left(\frac{D_{1o}}{D_{2i}} + 1\right)}$$

$$b = \frac{(2-a)(9\gamma - 5)}{2a(\gamma + 1)}$$

$$\lambda = \frac{2.331 \times e^{-20}(T_{g12} + 273.15)}{P_a \delta^2}$$

Where

D_{1o} = outer surface diameter of 1^{st} glass cover (m)

D_{2i} =inner surface diameter of 2^{nd} glass cover (m)

h_{12} =convection heat transfer coefficient for the annulus air at $T_{g12}(W/m^2 - K)$

$T_{g_{1o}}$ =outer surface temperature of 1^{st} glass cover $(^\circ C)$

$T_{g_{2i}}$ =inner surface temperature of 2^{nd} glass cover $(^\circ C)$

k_{std} =thermal conductance of the annulus gas at standard temperature and pressure $(W/m - K)$

b = interaction coefficient

λ =mean-free-path between collisions of a molecule (cm)

a = accommodation coefficient

γ =ratio of specific heats for the annulus gas

T_{g12} =average temperature $(T_{g_{1o}} + T_{g_{2i}})/2 \quad (^\circ C)$

Pa =annulus gas pressure (mm of Hg)

δ =molecular diameter of annulus gas (cm)

The molecular diameters, δ, of the air as well as other gases like hydrogen and argon were obtained from Marshal (1976) [159] and are shown in Table 4.2. The table also compares the convection heat transfer coefficients (h_{12}) and other parameters that are used in the calculation for different gases included in the helical coil solar cavity receiver performance model.

Table 4.2: Heat Transfer Coefficients and Constants for Each Annulus Gas[158]

Constants	Air	Hydrogen	Argon
k_{std}	0.02551	0.1769	0.01777
b	1.571	1.581	1.886
λ	88.67	191.8	76.51
γ	1.39	1.398	1.677
δ	$3.53 \times e^{-8}$	$2.4 \times e^{-8}$	$3.8 \times e^{-8}$
h_{12}	0.0001115	0.0003551	0.00007499

When the pressure between 1^{st} and 2^{nd} glass covers is greater than 133.322 Pa then the convection heat transfer mechanism between the 1^{st} and 2^{nd} glass cover occurs by natural convection. Raithby and Holland's correlation for natural convection in an annular space is used for this case Bejan (1995) [160]. This correlation assumes long, horizontal, concentric cylinders at uniform temperatures, and is valid for $Ra_{D2i} \geq (D_{2i}/(D_{2i}–D_{1O}))^4$. All physical properties are evaluated at the average temperature $(T_{g_{1o}} + T_{g_{2i}})/2$

$$Q_9 = \frac{2.425 k_{12} \left(T_{g_{1o}} - T_{g_{2i}}\right) \left(Pr \times \frac{Ra_{D_{1o}}}{0.861 + Pr_{12}}\right)^{1/4}}{\left(1 + \left(\frac{D_{1o}}{2i}\right)^{3/5}\right)^{5/4}} \tag{4.21}$$

$$Ra_{D1o} = \frac{g\beta \left(T_{g_{1o}} - T_{g_{2i}}\right) D_{1o}^3}{\nu\alpha} \tag{4.22}$$

where

D_{1o} = outer surface diameter of 1^{st} glass cover (m)

D_{2i} = inner surface diameter of 2^{nd} glass cover (m)

k_{12} = thermal conductance for the annulus air at $T_{g_{12}}$ W/m-K)

$T_{g_{1o}}$ = outer surface temperature of 1^{st} glass cover (^oC)

$T_{g_{2i}}$ = inner surface temperature of 2^{nd} glass cover (^oC)

T_{g12} = average temperature $(T_{g_{1o}} + T_{g_{2i}})/2$ ($^\circ C$)

β = volumetric thermal expansion coefficient $(1/K)$

Pr_{12} = Prandtl number

Ra_{D1O} = Rayleigh number evaluated at D_{1O}

$\beta = 1/T_{g_{12}}$

4.1.8.2 Radiation Heat Transfer (Q_{10})

The radiation heat transfer between the 1^{st} and 2^{nd} glass is estimated with by using the equation (4.23) suggested by Incropera and DeWitt (1990).

$$Q_{10} = \frac{\sigma \pi D_{1o} \left(T_{g_{1o}}^4 - T_{g_{2i}}^4\right)}{\frac{1}{\varepsilon_{g1o}} + \frac{D_{1o}}{D_{2i}} \left(\frac{1-\varepsilon_{g_{2i}}}{\varepsilon_{g_{2i}}}\right)} \tag{4.23}$$

where

Q_6 = convection heat transfer between receiver and 1^{st} glass cover per unit length of receiver

d_o = absorber outside diameter (m)

T_3 = absorber outside surface temperature (K)

$T_{g_{1i}}$ =inner surface temperature of 1^{st}glass cover (K)

4.1.9 Heat Transfer from the 2nd Glass Cover to Atmosphere

The heat will transfer from the 2^{nd} glass cover to the atmosphere by convection and radiation. The convection heat transfer will either be forced or natural, depending on whether there is wind or no wind. Radiation heat loss occurs due to the temperature difference between the 2^{nd} glass cover and the sky.

4.1.9.1 Convection Heat Transfer (Q_{12})

The convection heat transfer from the glass envelope to the atmosphere is the major source of heat loss, especially if there is a wind. From Newton's law of cooling

$$Q_{12} = h_{2ga} \pi D_{2o} \left(T_{g_{2o}} - T_a\right) \tag{4.24}$$

$$h_{2ga} = \frac{k_{g_{2a}}}{D_{2o}} Nu_{D_{2o}} \tag{4.25}$$

where

Q_{12} = convection heat transfer from 2^{nd} glass cover to ambient per unit length

D_{2o} = outer diameter (m) of 2^{nd} glass cover

Tg_{2o} = outer surface temperature of 2^{nd}glass cover ($^{\circ}C$)

T_a = ambient temperature ($^{\circ}C$)

h_{2ga} = convection heat transfer coefficient for air at $(T_{g_{2o}}–T_a)/2$ (W/m^2-K)

Nu_{D2o} = average Nusselt number based on the glass envelope outer diameter

The Nusselt number depends on whether the convection heat transfer is free convection (no wind) or forced convection (with wind).

4.1.9.2 Free Convection (no wind case)

If there is no wind, the convection heat transfer from the 2^{nd} glass cover to the environment will be take place by free convection. In this case, the correlation developed by Churchill et al [161] will be used to estimate the Nusselt number. This correlation is valid for $10^5 < Ra_{Dg2o} < 10^{12}$, and assumes a long isothermal horizontal cylinder. Also, all the fluid properties are determined at the film temperature, $(T_{g2o}+T_a)/2$. In the present experimental setup outer glass cylinder is of finite length (assume long) with relatively small temperature gradient (assume isothermal surface) along its length. However, any errors associated with the assumptions should be relatively small.

$$Nu_{D_{g_{2o}}} = \left\{ 0.60 + \frac{0.387 Ra_{D_{g_{2o}}}^{1/6}}{\left[1+\left(\frac{0.559}{Pr_{g_{2a}}}\right)^{9/16}\right]^{8/7}} \right\}^2 \tag{4.26}$$

$$Ra_{D_{g2o}} = \frac{g\beta\left(T_{g_{2o}}-T_a\right)\times D_{g_{2o}}^3}{\alpha_a \nu_a} \tag{4.27}$$

$$\beta = 1/T_{g_{2a}} \tag{4.28}$$

$$Pr_{g_{2a}} = \frac{\nu_a}{\alpha_a} \tag{4.29}$$

where

$Ra_{Dg_{2o}}$ = Rayleigh number for air based on the 2nd glass cover outer diameter,

$D_{g_{2og}}$ = gravitational constant (9.81 m/s^2)

α_a = thermal diffusivity for air at $T_{g_{2a}}(m^2/s)$

β =volumetric thermal expansion coefficient (ideal gas) $(1/K)$

$Pr_{g_{2a}}$ = Prandtl number for air at $T_{g_{2a}}$

υ_a =kinematic viscosity for air at $T_{g_{2a}}$ (m^2/s)

$T_{g_{2a}}$ = film temperature $(T_{g_{2o}} + T_a)/2$ (K)

4.1.9.3 Force Convection (wind case)

If there is wind, the convection heat transfer from the 2^{nd} glass cover to the environment will be taken place by forced convection. The heat transfer coefficient h varies with wind direction i.e. whether the flow of wind is along the length or across the length of helical coil solar cavity receiver. An equation which correlates the average heat transfer coefficient h_{2ga} over the circumference is given by Churchill and M. Bernstein [162] for external forced convection flow normal to an isothermal cylinder.

$$\bar{Nu}_{D_{2o}} = \frac{\bar{h}_{g_{2a}} D_{2o}}{k} = 0.3 + \frac{0.62 Re_{D_{2o}}^{1/2} Pr^{1/3}}{\left[1 + \left(\frac{0.4}{Pr}\right)^{2/3}\right]^{1/4}} \left[1 + \left(\frac{Re_{D_{2o}}}{282000}\right)^{5/8}\right]^{4/5} \tag{4.30}$$

Valid for: flow normal to glass cover$Pe = Re_{D_{2o}} Pr \geq 0.2$ properties at the film temperature(T_f)

where $Re_{D_{2o}}$ is the Reynolds number based on diameter D_{2o} of 2^{nd} glass envelope and Pe is the Peclet number defined as the product of the Reynolds and Prandtl numbers. For $Pe < 0.2$, the following is used which is suggested by Nakai and Okazaki [26]

$$\bar{Nu}_{D_{2o}} = \frac{\bar{h}_{g_{2a}} D_{2o}}{k} = \frac{1}{0.8237 - 0.5Pe} \tag{4.31}$$

Valid for: flow normal to glass cover $Pe = Re_{D_{2o}} \times Pr \leq 0.2$ properties at the film temperature (T_f)

4.1.9.4 Radiation Heat Transfer (Q_{13})

Radiation heat transfer between the 2^{nd} glass cover of helical coil solar cavity receiver and sky which has been discussed here is caused by the temperature difference between the glass cover and sky. Here, the glass cover is assumed to be a small convex gray object inside a large blackbody cavity (sky). The sky, especially during the cloudy conditions, does not act like a blackbody; however, it is common practice to model it as such the effective sky temperature is approximated as being $8°C$ below the ambient temperature Duffie and Beckman (1991) [163]. The net radiation heat transfer between the glass cover and sky has been calculated using the equation (4.32).

$$Q_{13} = \sigma D_{2o} \pi \varepsilon_{g_{2o}} \left(T_{g_{2o}} - T_s\right) \tag{4.32}$$

where

σ = Stefan-Boltzmann constant (5.670×10^{-8}) $(W/m^2 - K^4)$

$D_{2o} = 2^{nd}$ glass outer diameter (m)

ε_{g2o} = emissivity of the 2^{nd} glass cover outer surface

$T_{g2o} = 2^{nd}$ glass cover outer surface temperature (K)

T_s = effective sky temperature $(K) = T_a - 8$

4.1.10 Heat Loss through Supporting Rod and Bracket

Other sources of thermal losses are support bracket and supporting rod. In the present experimental setup, there are two supports: first one is the thick rectangular aluminium rod to support the helical coil so that the transverse deflection of helical coil could be protected and second is the bracket made up of plain carbon steel which is used to support complete receiver system. Some studies have not included the heat loss due to the support mechanism [164]. However, the place, where the solar field is spread over the large area of about $2 \times 10^5\, m^2$, the losses are significant and cannot be neglected [165]. In the present calculation, the bracket is assumed to be an infinitely long fin with base temperature $10°C$ less than that of the outer absorber surface temperature [124] and loss due to supporting

rod is assumed to be neglected. The losses from each bracket can be calculated using the equation (16.4) as:

$$Q_{a,b} = \left(\frac{Nu_b P_b k_b A_b}{D_b L_t}\right)^{0.5} (T_b - T_a) \tag{4.33}$$

In eq. (4.33), the suffix b stands for the bracket. The symbols P, k and A represent the perimeter (m), thermal conductivity ($W/m-K$) and minimum area of cross section (m^2) of bracket respectively. Nub is the average Nusselt number based on the bracket temperature, L_t is the total length of the receiver, T_b is the temperature at the base of the bracket ($^\circ C$).

4.1.11 Optical Properties

The optical properties used in the helical coil solar cavity receiver performance model were obtained from a combination of sources. There are many factors which has been shown in Table 4.3 [166]that affect the PTC performance model: geometric effects which includes shadowing due to support bracket, tracking error, and improper alignment of PTC system, mirror and glass cover transmittance effects which arise due to mirror reflectance, and dirt/dust on aperture as well as receiver (recommended by Duffie and Beckman (1991), and an another factor that can't be explain the differences between field test data and modeled data. One more term called incident angle modifier which accounts for incident angle losses. This factor is a function of the solar incidence normal to the collector aperture and is needed for the cases when the solar irradiation is not normal to the collector aperture. This factor was determined from the relation given in equation (4.34) Dudley et al. (1994) [163].

$$K = \cos(\theta) + 0.000884\theta - 0.00005369\theta^2 \tag{4.34}$$

where θ = solar incidence angle normal to the collector aperture

Table 4.3: Estimates of Effective Optical Efficiency Term[165]

Symbols	Factors	Value
$\acute{\varepsilon}_1$	Receiver shadowing	0.974
$\acute{\varepsilon}_2$	Tracking error	0.994
$\acute{\varepsilon}_3$	Geometry error	0.980
ρ_{c_1}	Clean mirror reflectance	0.935
$\acute{\varepsilon}_4$	Dirt/dust on mirror	$reflectivity/\rho_{c_1}$
$\acute{\varepsilon}_5$	Dirt/dust on glass cover	$(1+\acute{\varepsilon}_4)/2$
$\acute{\varepsilon}_6$	Unaccounted	0.96

*Reflectivity is the user input that depends on material/coatings. In parabolic trough concentrator typically its value lies between 0.88 to 0.93

4.1.12 Solar Irradiation Absorption in the 2nd Glass Cover (Q_1)

The solar absorption into the glass cover is treated as a surface phenomenon to simplify the model. Practically this is not true. The solar radiation absorbed by the glass cover is a heat generation phenomenon and it depends on glass thickness. However, this assumption introduces negligible error due to small absorptivity (0.02) and thickness (2.5mm) of glass cove Touloukian and DeWitt (1972). The equation for the solar absorption in the 2^{nd} glass cover becomes

$$Q_1 = Q_{si}\eta_{2gc}\alpha_{2gc} \tag{4.35}$$

with

$$\eta_{2gc} = \varepsilon_1^{'}\varepsilon_2^{'}\varepsilon_3^{'}\varepsilon_4^{'}\varepsilon_5^{'}\rho_{c_1}K \tag{4.36}$$

whereQ_{si} = solar irradiation on 2^{nd} glass cover per unit length (W/m)

η_{2gc} =effective optical efficiency at the 2^{nd} glass cover

α_{2gc} =absorptance of the 2^{nd} glass cover (Borosilicate glass)

K =incident angle modifier

The values of all terms in Equation 4.36, except for K, are from Table 4.3. The solar irradiation (Q_{si}) in Equation 4.36 is determined by multiplying the direct normal solar radiation intensity by the projected normal reflective surface area of the collector (aperture area) and dividing by the length of 2^{nd} glass cover. All terms used in equations 4.35 and 4.36 are assumed to be independent of temperature.

4.1.13 Solar Irradiation Absorption In the 1st Glass Cover (Q_2)

$$Q_2 = Q_{si}\eta_{1gc}\alpha_{1gc} \tag{4.37}$$

with

$$\eta_{1gc} = \eta_{2gc}\tau_{2gc} \tag{4.38}$$

where

Q_{si} = solar irradiation on 1^{st} glass cover per unit length (W/m)

η_{1gc} = effective optical efficiency at the 1^{st} glass cover

α_{1gc} = absorptance of the 1^{st} glass cover (Borosilicate glass)

τ_{2gc} = transmittance of the 2^{nd} glass cover

4.1.14 Solar Irradiation Absorption in the Absorber (Q_3)

$$Q_2 = Q_{si}\eta_{abs}\alpha_{abs} \tag{4.39}$$

$$\eta_{abs} = \eta_{1gc}\tau_{1gc} = \eta_{2gc}\tau_{2gc}\tau_{1gc} \tag{4.40}$$

where

Q_{si} = solar irradiation on helical coil receiver per unit length (W/m)

η_{1gc} = effective optical efficiency at the 1^{st} glass cover

η_{2gc} = effective optical efficiency at the 2^{nd} glass cover

α_{1gc} = absorptance of the $1st$ glass cover (Borosilicate glass)

τ_{2gc} = transmittance of the2^{nd} glass cover

τ_{1gc} = transmittance of the 1^{st} glass cover

4.1.15 Exegetic Modeling

The exergetic output is one of the most important parameters in the analysis of solar collector. Exergy represents the work potential of any process and is equal to the useful heat minus the irreversibilities [167]. The exergetic analysis of the solar collector includes the three main points under study (a) exergy of the solar radiation (b) the useful exergy production (c) the exergetic losses and (d) the exgergetic destruction. Parabolic trough concentrator technology utilize only direct solar radiation for their performance and is assume to be undiluted [168]. In the present exergetic analysis the sun is assume to be the radiation reservoir not the heat reservoir with a surface temperature of $5770\,K$ and estimating the exergy flow of incoming solar radiation as suggested by the Petela model [169]. The exergetic output of solar collector can be calculated according to the eq. (4.41) [170]

$$E_u = Q_u - \dot{m}c_p T_a \ln\left(\frac{T_e}{T_i}\right) - \dot{m}T_a\left[\frac{\Delta P}{\rho T_{fm}}\right] \tag{4.41}$$

Eq. (4.41) shows clearly that the exergetic output of solar collector is equal to useful energy gain minus two quantities. The first quanty is related to the loss of ideal heat transfer due to irreversibility while the second term accounts for the pressure loss along the tube. Second term depends upon the characteristics of fluid flowing through the receiver. In the case of Eq. (4.41) shows clearly that the exergetic output of solar collector is equal to useful energy gain minus two quantities. The first quanty is related to the loss of ideal heat transfer due to irreversibility while the second term accounts for the pressure loss along the tube. Second term depends upon the characteristics of fluid flowing through the receiver. In the case of gaseous working fluid, pressure loss across the tube is considerable due to low density and hence this term is significant in this case. But if the working fluid is liquid as in the present experimental work, the last term of eq. (4.41) may be neglected and equation reduced to eq.(4.42).

$$E_u = Q_u - \dot{m}c_p T_a \ln\left(\frac{T_e}{T_i}\right) \tag{4.42}$$

The rate of solar exergy is a much discussed issue in the present scenario. Usually, sun is treated as a thermal energy reservoir but according to Petela theory [169], the sun is a radiative reservoir and the exergetic flow rate has been found out as under:

$$E_s = Q_s \left[1 - \frac{4}{3} \left(\frac{T_a}{T_{sun}} \right) + \frac{1}{3} \left(\frac{T_a}{T_{sun}} \right)^4 \right] \tag{4.43}$$

Exergetic efficiency is defined as the ratio of exergetic output to the solar exergy flow rate and can be determined using the equation (4.44) [171]

$$\eta_{ex} = \frac{E_u}{E_s} \tag{4.44}$$

Exergy losses and exergy destruction are very important parameters to be calculated in order to perform a complete exergetic analysis of solar collector. Exergy losses (E_{loss}) are defined as the heat losses of the system under study which cannot be utilized or recovered further. These losses include the optical and thermal losses. Optical, thermal and total exergetic losses can be calculated using the eqs. (4.45) - (4.47) as:

$$E_{loss,opt} = (1 - \eta_{abs}) E_s \tag{4.45}$$

$$E_{loss,th} = Q_{loss} \left(1 - \frac{T_a}{T_r} \right) \tag{4.46}$$

Total exergetic losses have been given as:

$$E_{loss} = E_{loss,pot} + E_{loss,th} \tag{4.47}$$

Exergy destruction implies the irreversibility during the course of heat transfer. Solar radiation coming from sun first absorbed by helical coil receiver and then the absorbed heat is transfer to the heat transfer fluid. Exergy destruction phenomena of solar radiation occur in two cases. The first one is between sun and receiver and second between receiver and heat transfer fluid. The total exergy destruction (E_d) can be calculated using the

eq.(4.47) [168][14] as:

$$E_d = \left[\eta_{abs}E_s - Q_{abs}\left(1-\frac{T_a}{T_r}\right)\right] + \left[Q_u\left(1-\frac{T_a}{T_r}\right) - E_u\right] \tag{4.48}$$

4.1.16 Pressure Drop Across the Helical Coil Solar Cavity Receiver

The pressure drop along the length of solar receiver is only the undefined parameter that needs to be defined up to the present analysis. This parameter has the significant effect on the exergetic performance of the system. The great values of pressure drop along the length of receiver lead to high energy consumption. The friction factor profile for the flow of thermal oil through the helically coiled receiver can be calculated using the Ito's laminar and turbulent resistance formulae [172]as:

$$f_{coil} = \frac{344\left(\frac{D}{d}\right)^{-0.5}}{\left[1.56+\log_{10}\left\{Re\left(\frac{D}{d}\right)^{-0.5}\right\}\right]^{5.33}} \tag{4.49}$$

Condition: $13.5\left(\frac{D}{d}\right)^{0.5} \leq Re \leq 2000\left[1+1.32\left(\frac{D}{d}\right)^{-0.6}\right] \cup 5 \leq \frac{D}{d} \leq 2000$

$$f_{coil} = 0.076Re^{-0.25} + 0.00725\left(\frac{D}{d}\right)^{-0.5} \tag{4.50}$$

Condition: $Re \geq 15000 \cup 5 \leq \frac{D}{d} \leq 2000$

Hence, pressure drop across the helical coil can be calculated using the eq. (4.51)

$$\Delta P = f_{coil}\frac{L}{d}\left(\frac{1}{2}\rho v^2\right) \tag{4.51}$$

Mean velocity (v) of flow can be determined using mass flow rate equation:

$$v = \frac{\dot{m}}{\rho\left(\frac{\pi}{4}d^2\right)} \tag{4.52}$$

The equations which have been presented under section 1.1 are the fundamental of the developed performance model. The present model calculates the optical, thermal and exergetic collector performance in various cases. This model, which is developed in EES

(Engineering Equation Solver), is validated with experimental results of the present experimental setup.

4.2 Modeling of Dish Type Solar Concentrator

4.2.1 Heat Transfer Equations

The schematic diagram showing the system has been shown in figure 4.4. The system in the present discussion has been analyzed on the basis of three chunks: receiving pot, cooking fluid and the air volume in the cooking pot. Ideally, heat transfer should be studied on these components only neglecting the losses; but for a dish type solar collector with cylidrical receiver the amount of heat loss is considerable and thus cannot be neglected. The cooking pot receives heat from the concentrator which focuses a part of the radiations falling on it. This heat is being absorbed by receiver material and then transferred to the working fluid and the air volume present in the cylidrical receiver. The rest is being lost to the atmosphere in form of convection and radiation. According to heat balance equation for the system:

$$Q_R = Q_f + Q_{loss} + m_R C_R \frac{\partial T_R}{\partial t} \tag{4.53}$$

where $Q_R = \alpha_R Q_d$

$$Q_d = \rho_d F_d \eta_d I_d A_d$$

$$Q_{ra} = h_a A_s (T_R - T_a)$$

Considering the working fluid, the heat absorbed by the working fluid is being utilized by it to raise its temperature and a part of it is being transferred to the air volume by convection (Q_{fa}).

$$Q_f = Q_{fa} + m_f C_f \frac{\partial T_f}{\partial t} \tag{4.54}$$

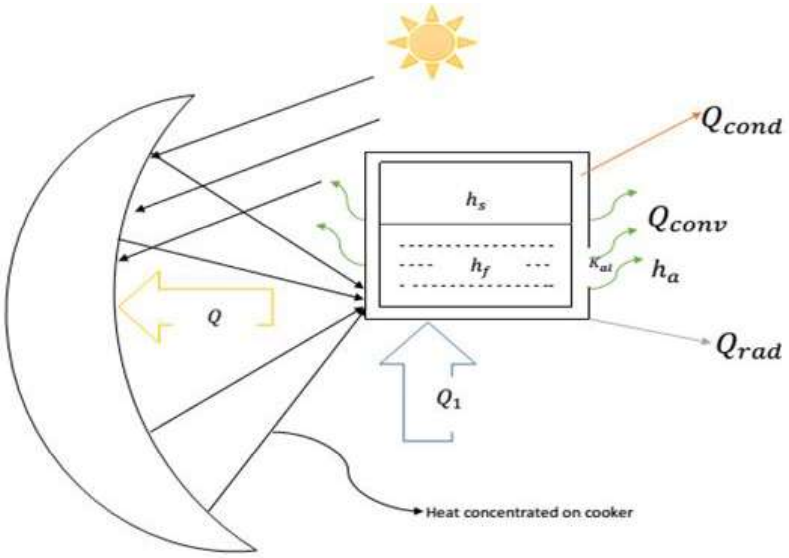

Figure 4.4: Schematic diagram showing the system and heat transfer

where $Q_{fa} = h_a A_a \left(T_f - T_a\right)$

Analysing the air volume in the cylidrical receiver as the system of study it can be seen that a part of the heat absorbed by the air volume is lost to the surrounding from the top (Q_{top}) and the left is utilized to increase the temperature of the air volume. Thus,

$$Q_{ra} + Q_{fa} = Q_{top} + m_a C_a \frac{\partial T_a}{\partial t} \tag{4.55}$$

where $Q_{top} = \frac{A_{top}(T_a - T_{amb})}{R_{top}}$; $R_{top} = \frac{1}{h_a} + \frac{x_t}{K_t}$

4.2.2 Loss Investigation

The losses from the system under study (cooker) can be studied by taking into consideration the different faces from which the loss takes place. The electrical analogy for the heat losses from the cooker is shown in figure 4.6.

4.2.2.1 Side Loss:

The losses occurring from the side or cylindrical surface of the cooker constitute the side loss. Losses occur from the cylindrical surface due to the temperature difference between

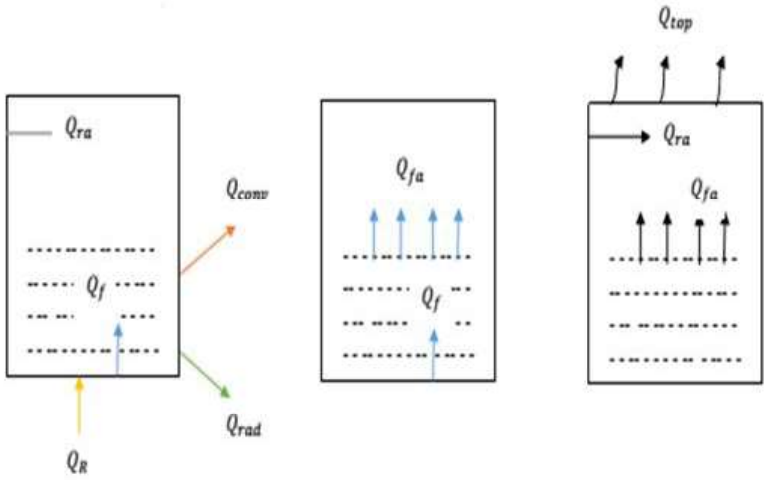

Figure 4.5: Schematic diagram showing various possible heat transfers

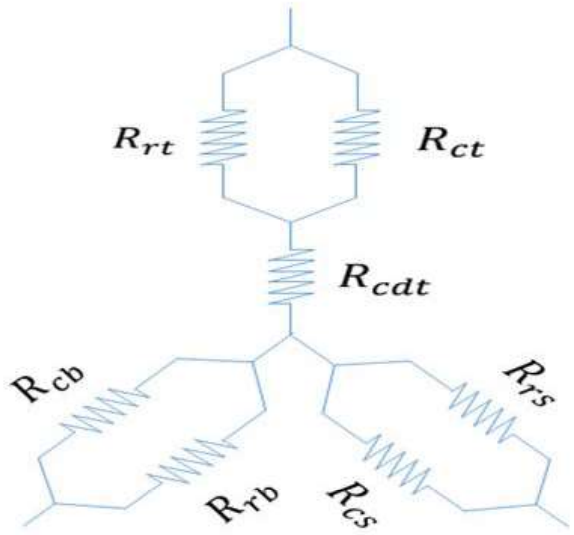

Figure 4.6: Electrical analogy of various losses for the parabolic dish type cooker

the fluid and ambient in form of convection and radiation.

Convection loss coefficient To incorporate the effect of wind in the heat loss calculation by convection, the heat transfer coefficient between the outer surface of cooker and ambient is computed using the relation mentioned in (Duffie and Beckmen 2013) for the cylindrical surface:

$$h_{cs} = 5.7 + 3.8V \quad (W/m^2K) \tag{4.56}$$

Radiation loss coefficient The cooker under study was painted with black matt on its surface to enhance its absorptivity.

It is known, $Q_{rs} = \varepsilon_{bm}\sigma\left(T_r^4 - T_{sky}^4\right) = h_{rs}\left(T_r - T_{sky}\right)$

thus

$$h_{rs} = \frac{\varepsilon_{bm}\sigma\left(T_r^4 - T_{sky}^4\right)}{T_r - T_{sky}} \tag{4.57}$$

The coefficient of radiative heat loss from cooker wall to ambient depends upon radiation exchange with the sky at sky temperature. $T_{sky} = T_{amb} - 6$

Calculating the side overall heat loss coefficient (U_s)

$$\frac{1}{U_s} = \frac{1}{h_{cs} + h_{rs}} \tag{4.58}$$

$$Q_s = U_s A_S (T_r - T_{amb}) \tag{4.59}$$

from equations (4.56), (4.57)and (4.58)

$$Q_s = \left[5.7 + 3.8V + \frac{\varepsilon_{bm}\sigma\left(T_r^4 - T_{sky}^4\right)}{T_r - T_{sky}}\right](T_r - T_{amb}) \times 2\pi R_c L_c \tag{4.60}$$

4.2.2.2 Bottom Loss:

The bottom surface is considered a flat surface and heat is lost from it due to convection and radiation.

Convection loss coefficient To incorporate the effect of wind velocity on convective heat transfer coefficient between the ambient and cooker base is being computed using the relation (Duffie and Beckmen 2013)

$$h_{cb} = 2.8 + 3.0V \tag{4.61}$$

Radiation loss coefficient Computing the radiation heat loss coefficient in the same way as calculated for the side loss in eq. 4.57

$$h_{rb} = \frac{\varepsilon_{bm}\sigma\left(T_r^4 - T_{sky}^4\right)}{T_r - T_{sky}} \tag{4.62}$$

Computing the bottom overall heat loss coefficient (U_b)

$$\frac{1}{U_b} = \frac{1}{h_{cb} + h_{rb}} \tag{4.63}$$

$$Q_b = U_b A_b (T_r - T_{amb}) \tag{4.64}$$

from equation 4.62, 4.63 & 4.64

$$Q_b = \left[2.8 + 3.0V + \frac{\varepsilon_{bm}\sigma\left(T_r^4 - T_{sky}^4\right)}{T_r - T_{sky}}\right](T_r - T_{amb}) \times 2\pi R_c^2 \tag{4.65}$$

4.2.2.3 Top Loss:

The top loss constitutes all the losses taking from the lid or the upper surface of the cylidrical receiver. It embraces the heat losses from air volume present above the liquid if the pot is not completely filled. Thus it includes the conduction loss across the lid of the cooking vessel.

Convection loss coefficient The coefficient heat loss coefficient is computed using eq. 4.61 for a flat surface

$$h_{ct} = 2.8 + 3.0V \tag{4.66}$$

Radiation loss coefficient The radiation loss coefficient is calculated in the same way as for the bottom part of the cylidrical receiver and is given by

$$h_{rb} = \frac{\varepsilon_{al}\sigma\left(T_r^4 - T_{sky}^4\right)}{T_r - T_{sky}} \tag{4.67}$$

From resistance analogy

$$R_{top} = \frac{1}{h_{ct} + h_{rt}} + \frac{x_t}{k_t} \tag{4.68}$$

$$Q_{top} = \frac{A_{top}(T_a - T_{amb})}{\frac{1}{h_{ct}+h_{rt}} + \frac{x_t}{k_t}} \tag{4.69}$$

Using relations (4.66-4.69)

$$Q_{top} = \frac{k_t\left[2.8 + 3.0V + \frac{\varepsilon_{al}\sigma\left(T_{ar}^4 - T_{sky}^4\right)}{Ta_r - T_{amb}}\right]}{k_t + x_t\left[2.8 + 3.0V + \frac{\varepsilon_{al}\sigma\left(T_{ar}^4 - T_{sky}^4\right)}{T_a - T_{amb}}\right]}(T_a - T_{amb}) \times \pi R_{top}^2 \tag{4.70}$$

4.2.2.4 Total Loss:

The total loss from the cooker can be calculated by summing up all the heat losses from the various surfaces.

$$Q_{loss} = Q_{top} + Q_s + Q_b \tag{4.71}$$

4.2.3 Performance Index (PI)

Performance Index (PI) can be defined as the ratio of useful energy which is actually gained by the working fluid inside the cooking pot to the amount of incident solar radiation falling on the concentrated system. The intensity of radiation falling on system is a function of time as apparent from the variation of intensity with time (figure 1.)

$$PI = \frac{Q_{useful}}{I(t)A_c} \tag{4.72}$$

4.2.4 Efficiency of Dish type collector (η)

The efficiency of the cooking pot can be calculated by using the relation

$$\%\eta = \frac{performance\,index}{concentration\,ratio} \times 100 \tag{4.73}$$

4.3 Model Validation

The performance model developed in this study is based on the heat transfer analysis. In this paragraph, the results of the developed performance model was compared with other experimental results to evaluate the accuracy of the present performance model. Table 4.4 shows the comparison of experimental results with the results obtained from numerical model includes the comparison results and percentage deviation was found to be equal to 1.71%. This comparison shows that the developed model gives accurate results for the heat transfer fluid Mythol Therm 500 oil with a small deviation. Table 4.5 shows the comparison of experimental results with SNL Test results (1994). This comparison shows the 9.317% increment in thermal efficiency of the present experimental setup as compared to the Sandiya National Laboratory Test results. Table 4.6 shows the comparison of results between the developed model and the experimental data. This comparison shows the error/uncertainty of 0.103 ± 0.952,which leads to the better accuracy of the model. Fig. 4.7 represent the comparison of the present results with SNL Test results for number of observations. Variation of thermal efficiency of the present parabolic trough collector with average temperature above ambient has been shown in fig. 4.8 An empirical relation has been established between thermal efficiency and average temperature above ambient which can be used in future for further analysis.

Table 4.4: Comparison of experimental results with the results obtained from numerical model

Authors	Empirical relations	Theoritical Nusselt Number	Theoretical convective heat transfer coefficient (W/m^2-K)	Experimental convective heat transfer coefficient (W/m^2-K)	Experimental Nusselt Number	Percentage Deviation
Roger et al. [173]	$Nu = 0.023Re^{0.85}Pr^{0.4}\delta^{0.1}$	60.96	2012	1547	46.89	1.71%
M.R. Salimpour [146]	$Nu = 0.152De^{0.431}Pr^{1.06}\gamma^{-0.277}$	1289	42524			
Kalb et al. [174]	$Nu = 0.836De^{0.5}Pr^{1.0}$	28.86	952.3			
Xin et al. [175]	$Nu = (2.153+0.318De^{0.643})Pr^{0.17}$	46.1	1521			
Janssen and Hoogenwdoom [176]	$Nu = 0.7Re^{0.43}Pr^{\frac{1}{6}}\delta^{0.07}$	29.72	980.9			

Table 4.5: Present experimental results versus SNL Test results (1994)

Beam Radiation (W/m^2)	Inlet temp. (^oC)	Outlet temp. (^oC)	Receiver temperature (^oC)	Mean fluid temp. (^oC)	Thermal efficiency (ηth)	Thermal Efficiency (ηth) TEST- 2(1994)	Average increment in thermal efficiency (%)
766	61.5	61.5	65.5	57.4	86.53	72.51	9.317
746	55.4	55.4	61.5	52.25	68.26	67.91	
765	54.6	54.6	58	50.25	91.92	72.63	
739	63.5	63.5	67	60.35	68.46	63.82	
734	66.7	66.7	68	63.8	63.45	62.34	
878	58	58	61.5	54.15	70.89	70.25	
858	70.3	70.3	71.5	66.8	74.65	72.51	
671	56.8	56.8	59.5	52.9	93.96	70.9	

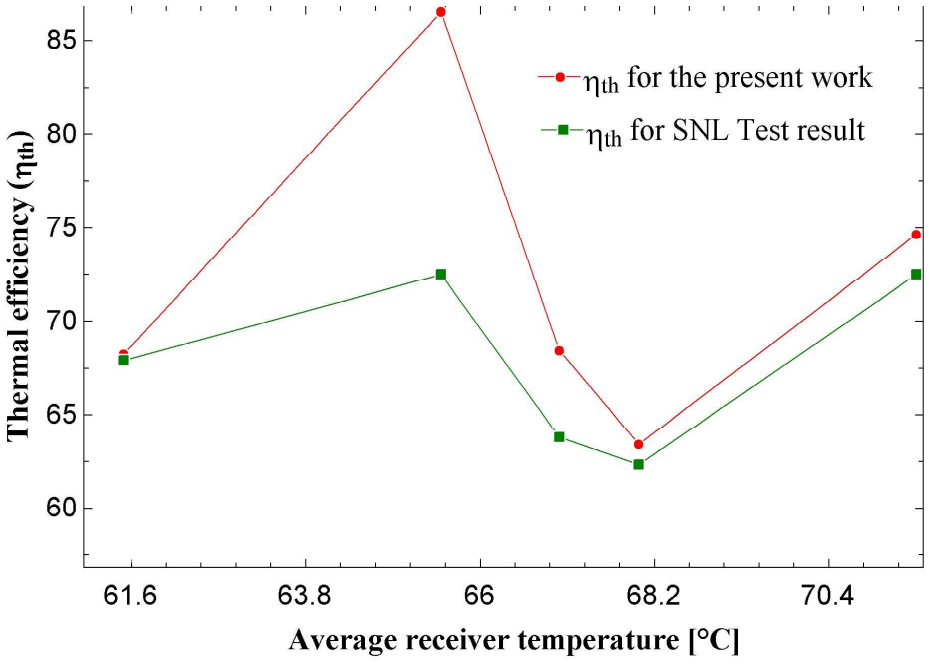

Figure 4.7: Comparison of thermal efficiencies between the present work and the SNL test results

Table 4.6: Performance model results versus experimental results

S.N	Test Date 2017	Direct Normal (W/m^2)	Wind Speed	Wind Direction	Air Temp. (^oC)	Temp. Inlet	Flow Rate	Temperature Outlet (^oC)		Deviation	Error/Uncertainty
								Experimental	Model		
01	11.04.2017	878	3.7	310	34.9	50.3	5.88	58	57.77	-0.2279	0.103 ± 0.952
02	14.04.2017	749	0.6	341	36.8	54.5	5.88	60.2	59.74	-0.4645	
03	15.04.2017	729	2.8	72	40.7	61	5.88	67.2	66.24	-0.9645	
04	17.04.2017	739	0.7	189	34.5	57.2	5.88	63.5	63.96	0.4604	
05	27.04.2017	766	0.7	312	37.8	53.3	5.88	61.5	61.53	0.03453	
04	02.05.2017	826	0.9	206	37.5	56.6	5.88	63.1	64.89	1.785	

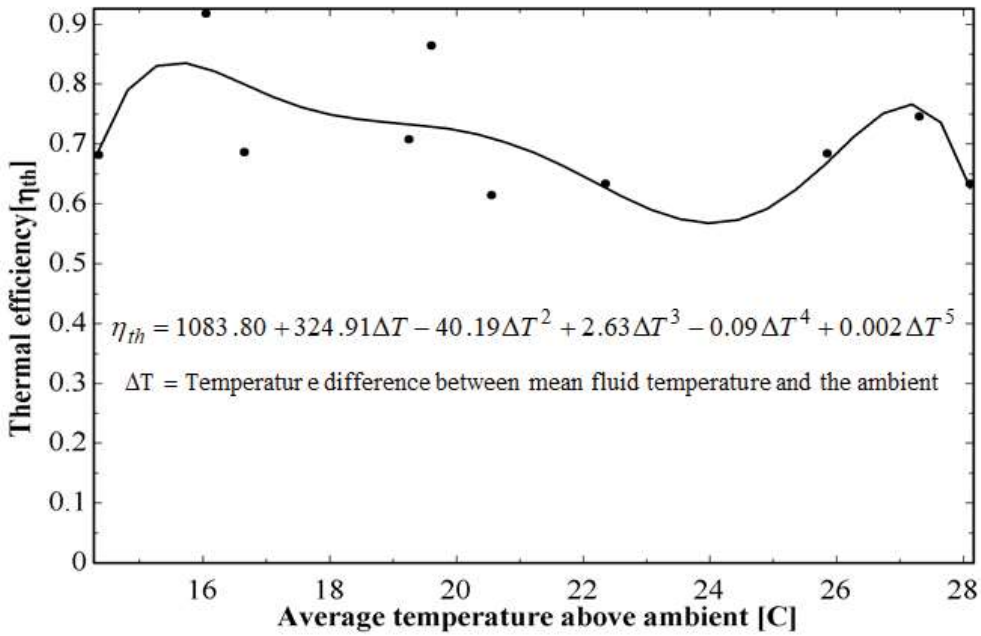

Figure 4.8: Variation of thermal efficiency of the present experimental setup with fluid temperature above ambient